Erschienen in: Proceedings of the 28th European Photovoltaic Solar Energy Conference and Exhibition (EU PVSEC 2013) ; Paris, France ; conference 30 September - 04 October 2013. - München : WIP, 2013. - S. 1659-1664. - ISBN 3-936338-33-7
https://dx.doi.org/10.4229/28thEUPVSEC2013-2CV.4.7

COMPARISON OF THE RECOMBINATION VELOCITY AT GRAIN BOUNDARIES GAINED BY LOCK-IN THERMOGRAPHY AND LIGHT BEAM INDUCED CURRENT MEASUREMENTS

Sven Rißland[1,*], Gabriel Micard[2], Otwin Breitenstein[1], Annika Zuschlag[2], Sven Seren[2], Barbara Terheiden[2], Giso Hahn[2]
[1] Max Planck Institute of Microstructure Physics, Weinberg 2, 06120 Halle, Germany
[*] Tel.: +49(0) 345 5582 692, Fax: +49(0) 345 5511 223, E-mail: rissland@mpi-halle.mpg.de
[2] Department of Physics, University of Konstanz, 78457 Konstanz, Germany

ABSTRACT: The surface recombination velocity at grain boundaries can be evaluated by means of Dark Lock-in Thermography (DLIT) or Light Beam Induced Current measurements (LBIC). In this contribution for a first time we apply both methods to the same grain boundaries and compare the results to each other. In spite of the quite similar models, which are the basis of both evaluations, there are quite strong differences in the required interpretation of both approaches. A detailed discussion presents the main issues in comparing recombination parameters of grain boundaries obtained from the different measurements and exposes that the used model represents the LBIC-based method better, but the DLIT-based evaluation proposes a better estimation of the influence of the GB on the solar cell performance. This is possible since DLIT provides a direct measurement of the dark current density caused by the recombination at the grain boundary, whereas the LBIC-based method is mainly sensitive to the recombination in the bulk. For this reason both methods may give similar results under strict limitations, but in some cases the DLIT method cannot be used to calculate a surface recombination velocity at the GB as it is defined in the underlying model.
Keywords: grain boundary, recombination, characterization, lock-in thermography, LBIC

1 INTRODUCTION

Todays silicon solar cells are mainly produced from multicrystalline (mc) silicon. These solar cells include a lot of crystal defects such as dislocations and grain boundaries, which induce different degrees of recombination activity. Increasing the performance of such solar cells requires a detailed understanding of the recombination effects lowering the efficiency. Recombination active grain boundaries (GBs) are one of the main origins of locally decreased effective carrier lifetimes and thus of an increased local diffusion current density. Amongst the various approaches, the evaluation of the recombination activity at the GBs in terms of a surface recombination velocity v_s can be performed using light beam induced current (LBIC) measurements [1] as well as dark lock-in thermography (DLIT) [2,3]. In this contribution we compare these two different approaches and present an interpretation of the obtained results. Therefore, both methods are applied to one and the same GB in two mc silicon solar cells, which are taken from neighboring wafers, but are processed slightly differently.

2 SAMPLE PREPARATION

In order to investigate the recombination activity of the grain boundaries with a limited influence of other crystal defects such as dislocations and extended crystal defects, which might be decorated with impurities, the samples are made from mc float-zone (FZ) material, grown from a mc seed crystal. This results in a very pure material quality with respect to a typical mc grain structure. The doping concentration of the samples is about 8.7×10^{15} cm^{-3}.

A laboratory-scale solar cell process was used, which is based on photolithography and is described in [4]. Two samples were investigated in this contribution, which are made from neighboring wafers with slightly different processing. Sample A was processed with a hydrogen passivation via SiN_x firing of the antireflection coating and sample B without this process step. Thus the recombination activity at similar GBs might be different, which enables an appropriate comparison of both methods of interest. The measured current-voltage (*I-V*) data of the 2×2 cm^2 sized solar cells are given in Table I.

Table I: Measured and simulated *I-V* data of mc-FZ solar cells (2×2 cm^2).

Sample		SiN_x firing	FF [%]	V_{oc} [mV]	j_{sc} [mA/cm^2]	η [%]
A	meas.	yes	79.3	599	33.7	16.0
	sim.*		78.0	598	33.7†	15.7
B	meas.	no	76.5	551	21.4	9.0
	sim.*		72.1	548	21.4†	8.5

* simulated by "Local I-V" from DLIT with RESI-R_s [5]
† taken as constant for the simulation

3 METHODS AND EXPERIMENTS

The recombination active GBs are attractive for minority charge carriers in their surrounding, since the recombination lowers the minority carrier concentration nearby. Thus the carriers, which were generated in the bulk by illumination or which are injected by an external bias, diffuse towards the recombination active GB and recombine there at a certain rate per unit surface. Normalizing this rate by the excess carrier density close to the GB gives the surface recombination velocity v_s that is a measure for this recombination process. In the simplest model this GB is perpendicular to the surface of the solar cell and homogeneous in depth. The diffusion of the minority charge carriers towards the GB is mainly characterized by the local diffusion length (L_{diff}). Both methods used in this contribution are based on such a model of a vertical GB in an infinitely thick solar cell with neglected recombination in the emitter and the depletion region. Beside this similarity the evaluation of v_s and L_{diff} is very different due to the different kind of excitation and the measured signal.

3.1 LBIC-based evaluation

Beam induced current measurements are able to detect a decreased current density reaching the contact in the surrounding of such recombination active structures due to the loss of charge carriers. For that purpose the evaluation of the surface recombination velocity of grain boundaries by means of LBIC requires a linescan perpendicular to the GB. First overview maps of the internal quantum efficiency (IQE) were measured (see Fig. 1(a) and (b)) and additional high resolution LBIC maps with two different lasers (833 and 910 nm) were measured in the region of interest. [4]

By normalizing the linescan to the level, which is measured infinitely far from the GB (plateau level), the so-called contrast profiles are obtained. An LBIC profile model considering the Gaussian excitation profile of the lasers enables the determination of v_s at the GB as well as the diffusion length of the minority carriers within the adjacent grains. This model, which is based on the solution of the carrier continuity equations and which is described in [6], also allows the consideration of the asymmetry in profiles due to different L_{diff} within the neighboring grains [1] and thus enables a quite general evaluation of grain boundaries. For simplicity and since the LBIC contrast profile is just weakly sensitive to these effects, the model neglects all recombination within the emitter and the depletion region and assumes an infinitely thick solar cell.

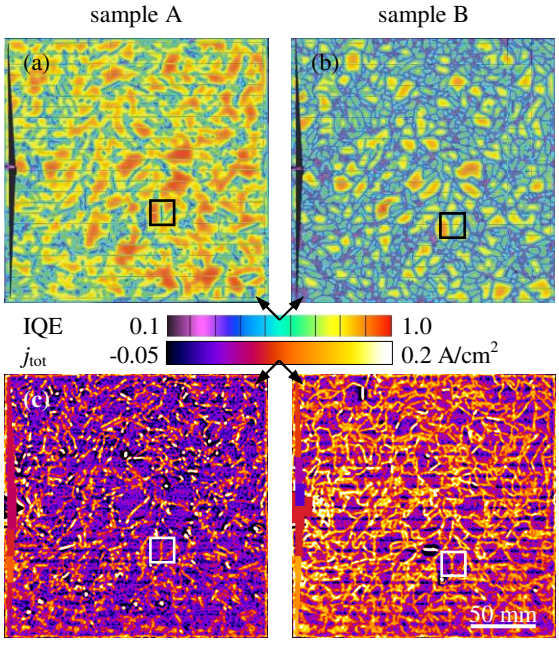

Figure 1: (a) and (b) internal quantum efficiency (at 980 nm), (c) and (d) total dark current density (at 600 mV) of solar cells made from neighboring mc FZ wafers, with (sample A) and without (sample B) hydrogenation via SiN_x firing.

3.2 DLIT-based evaluation

Dark lock-in thermography enables a direct measurement of current densities due to the diffusion of charge carriers caused by recombination activity of the GBs. The solar cell was sucked to a temperature-controlled chuck by a transparent foil and is biased by a four-probe contacting scheme. The IR-emissivity is evaluated from topography images at two different temperatures and corrected after the measurements [7].

In order to achieve an appropriate spatial resolution for the investigation the thermal blurring effect within the measured DLIT results has to be suppressed by a deconvolution algorithm. It has been shown in [2] that a complex 2-dimensional FFT-algorithm accomplish this. Figures 1(c) and (d) show the results of the deconvolution of DLIT results determined at a frequency of 23.4 Hz with an overall acquisition time of 15 hours each. This long measurement period yields in a very good signal-to-noise ratio and thus facilitates the FFT-algorithm.

Additionally the so-called Wiener filter is used within the deconvolution to control the influence of the residual noise on the result by a factor K [7]. Preliminary investigations suggest that a low K-factor in combination with a moderate Gaussian blurring of the results supresses the noise pattern and unpreventable undershooting of the deconvoluted signal next to power sources best and does not adulterate the result. For this reason the investigations were made using K = 1 and an additional Gaussian blurring with a radius of 1.5 px (equals 75 µm). Thus the full with at half maximum (FWHM) of the grain boundaries signal could be reduced to about 160 µm.

The separation of the dark current contributions according to the widely accepted two-diode model from DLIT measurements can be performed by the algorithm "Local I-V" [8]. For this purpose DLIT measurements at different biases are necessary, which enable an evaluation of the current-voltage characteristic at each point of the device. Since the deconvolution algorithm is very sensitive to noise, especially in the low signal regions within high lifetime grains, the resulting power source distribution is very spotted. According to the statistical noise of the measurement the corresponding pattern of the deconvoluted power distribution slightly differs in each measurement and thus a clear separation of the different dark current contributions in this region is not possible by "Local I-V", since the power distribution are not perfectly spatially aligned to each other. For this reason and since it is the dominant current contribution in the region of interests, the current density at 600 mV is evaluated as a simple diffusion current density without injection-level dependence. For the "Local I-V" analysis an R_s-image is necessary. This was calculated by the so-called RESI method [5] from the distribution of the local voltage U_{loc}, which was obtained from electro-luminescence (EL) images at 500 and 600 mV, which were evaluated by the algorithm "EL-Fit" [9].

Similar to the evaluation by means of LBIC, linescans perpendicular to the GB are measured in order to achieve a diffusion current density profile of the GB. Since the spatial resolution of our DLIT measurement is limited to 50 µm, several parallel linescans were averaged. Two parameters can be extracted using a Gaussian fit, which are the additional current line density J_{01}^{line} (the area underneath the curve) as well as the background value j_{01}^{back} (the baseline value), which describes the properties of the adjacent grain. The used equation (1) to determine v_s from these two values was developed on a model adopted from Lax [10] in a previous work of the authors [2] and was refined for low v_s in [3]:

$$v_s = \frac{j_{01}^{back} N_A}{q n_i^2} \cdot e \cdot \left[\exp\left(\frac{J_{01}^{line} \pi N_A}{2 D_n n_i^2 q} \right) - 1 \right] \qquad (1)$$

with the doping level $N_A = 8.7\times10^{15}$ cm^{-3}, the elementary charge q, Euler's number e, the intrinsic carrier density $n_i = 8.6\times10^9$ cm^{-3} at 25 °C and the minority carrier diffusion constant $D_n = 29.15$ cm^2/s. Another presentation of the equation is possible by applying the term: $j_{01}^{back} = D_n q n_i^2/(N_A L_{eff})$.

4 RESULTS

4.1 General influence of hydrogenation

The measurement of the internal quantum efficiency at 833 nm (Fig. 1(a) and (b)) clearly shows the influence of hydrogenation on recombination activity of the investigated solar cells. Sample B without the SiN_x firing has increased recombination velocities at most of the GBs as well as a decreased L_{diff} within the grains. This is also measured as an increased total current density by the DLIT measurements (Fig. 1(c) and (d)). A detailed analysis of the influence of hydrogenation on the GB's recombination activity by means of LBIC and EBIC investigations can be found in [4].

The "Local I-V" investigation of the primary results (not shown here) shows that the main contribution at 600 mV in the middle of the cell is caused by the diffusion current density j_{diff} and that the (depletion region) recombination current density j_{rec} is mainly located at the edges of the solar cells. The simulated values of the global data obtained from the local current density maps are also given in Table I and confirm that the procedure describes the parameters of the solar cell quite well. Nevertheless, the local investigation also points to the fact that the ratio of averaged j_{diff} to the averaged j_{rec} at 600 mV decreases due to the hydrogenation in the inner part of the solar cells. Thus there might be also some recombination within the depletion region at the GBs or within the grains, which is influenced by the H-passivation. Unfortunately the above described procedure does not provide a spatially high resolved separation of both current contributions due to the missing alignment of the noise pattern.

4.2 LBIC investigation at a selected GB

To obtain a detailed comparison of both methods a typical grain boundary next to a large grain with high L_{diff} is chosen, which is marked in Figure 1. This fact lowers the effect of a superimposed influence of different GBs on the measurement and thus supports the quantitative interpretation of the data. The high resolution LBIC images and enlarged DLIT maps of the same GB in the solar cells made from neighboring wafers are given in Figure 2.

The LBIC maps of Figure 2 are acquired with a spatial resolution of 2 µm in x and y. The horizontal lines (blue in the color scale) are the fingers of the front grid on which the signal is virtually zero due to the total reflection of the laser beam on the metal. The green/yellow lines in the color scale corresponds to the grain boundary on which the level is low but not zero because of the non-zero width of the laser beam and the finite recombination activity of these GBs. A linescan is taken simultaneously on the 833 nm LBIC map (dashed line in Figure 2) and on the 910 nm LBIC map not shown here. When normalized to the plateau level (level infinitely far in the left grain) it gives the contrast profile shown in Figure 3.

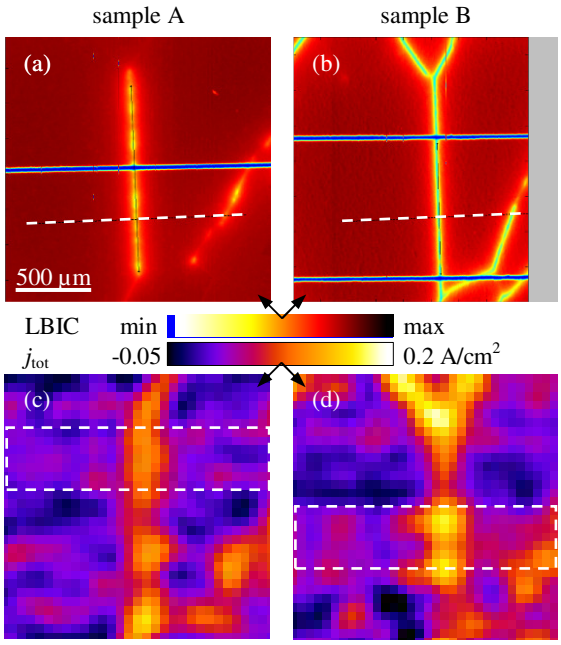

Figure 2: (a) and (b): High resolution LBIC map of the short circuit at λ = 833 nm. (c) and (d) detailed part of the total dark current density (at 600 mV) of sample A and B. The linescans used for the analysis are represented by the dashed lines resp. rectangles. The blue lines in the upper images belong to the metallization grid.

While the depth of the dip is directly linked to the v_s and to the width of the laser beam (measured independently), the width of the dip is linked to the diffusion length in the grain. The fact that the contrast profile of the 910 nm laser is broader and deeper than the 833 nm laser is a consequence of the fact that the former laser injects carriers deeper than the latter thus giving more opportunity for the injected carriers to recombine at the GB and in the bulk. The very good fitting of both linescans is a guarantee of the relevance of extracted v_s and L_{diff} value. However, due to the fact that the collection efficiency reaches almost unity for diffusion lengths above 900 µm, higher diffusion lengths induce only less than 1% change in the amplitude of the contrast and thus the determination of L_{diff} becomes inaccurate.

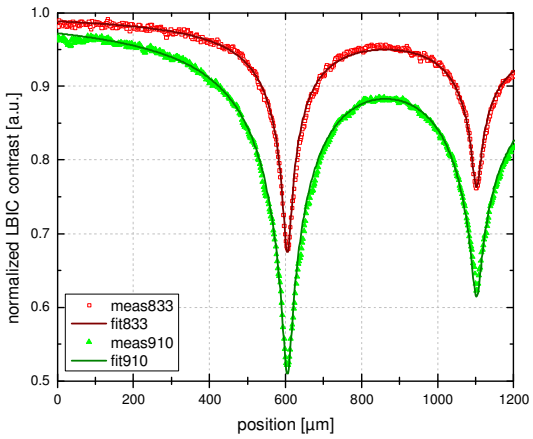

Figure 3: Fitting of the LBIC contrast profiles of sample A with laser wavelength 833 and 910 nm concerning the model presented in [1].

4.3 DLIT at selected GB

The spatial resolution of the DLIT data is limited to 50 µm/px due to the camera-based principle. A necessary emissivity correction of the measured DLIT data results in almost invisible gridlines within the primary images, but the thermal properties of the grid cannot be considered. Thus the signal in position of this gridlines is always slightly lower than in the surrounding area, which causes some artifacts in the deconvolution. For this reason these areas appear dark (with sometimes negative power densities) within the deconvoluted images as it is visible in Fig. 1(c) and (d) as well as in Fig. 2(c) and (d). They are neglected within the following analysis, since the linescans are taken in dashed marked region. These linescans are plotted in Figure 4.

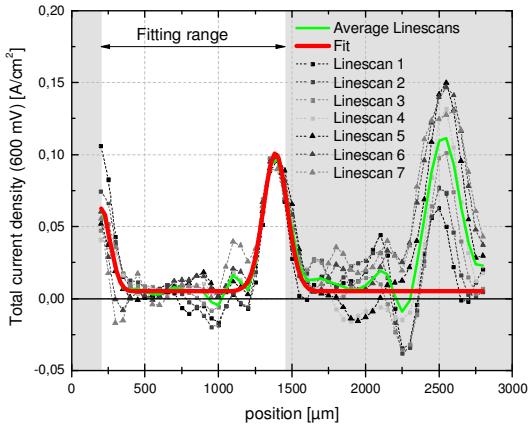

Figure 4: Fitting of the total current density linescans in sample A. The region of interest is marked by the dashed rectangle in Fig. 2(c)).

Since the DLIT model does not provide different properties of the grains at both sides of the GB, the fit was mainly limited to one side of the GB. If the GB is recombination active enough, there will be no exchange of carriers from one side towards the other and thus both sides can be interpreted separately [1]. The total current density is fitted to the averaged values of 7 linescans. The local voltage is constant to about ±0.5 mV and thus is not considered within the images, but is taken into account afterwards to calculate the saturation current densities from the measured total current densities at 600 mV. The uncertainty of the local voltage may cause an error in j_{01} of about ±4%, which is in the same range as the standard deviation of the averaged linescans. The resulting diffusion current density saturation values j_{01}^{back} of the grain and J_{01}^{line} characterizing the grain boundary are summarized in Table II for both samples. It is clearly visible that sample B has noise levels, which are almost twice as high as for sample A.

Table II: Extracted diffusion current densities at the GB measured by the evaluation of DLIT linescans.

Sample	j_{01}^{back} [A/cm²]	J_{01}^{line} [A/cm]
A	$(4.4 \pm 1.0)\times10^{-13}$	$(1.66 \pm 0.08)\times10^{-13}$
B	$(22.1 \pm 1.8)\times10^{-13}$	$(3.85 \pm 0.19)\times10^{-13}$

Calculating the surface recombination velocity of the investigated GBs by eq. (1) results in the values given in Table III. Due to the high noise in j_{01}^{back} of the high lifetime grain, the uncertainty of the values is quite high.

4.4 Comparison of both methods

Table III summarizes all results obtained from the evaluation of linescans by means of both above mentioned methods. The diffusion length L_{diff}, which is connected to the large grain at the left hand side of the GB, clearly increases due to hydrogenation. Thus the bulk becomes H-passivated. Both methods clearly show this trend, but the values obtained from DLIT are about a factor of 2 to 3 lower than measured by means of LBIC.

The recombination activity of the investigated GB clearly decreases due to the SiN_x firing. The evaluated v_s of sample A differs between both methods by a factor of about 30, while in sample B the DLIT evaluation regards a value, which is about 5 orders of magnitude higher than measured by LBIC. Since the thermal limit of v_s is about 2×10^7 cm/s, the values obtained by DLIT at sample B have not been evaluated correctly. Possible sources for this failing are discussed in the next section.

If the model of Lax [10] is used to evaluate the additional current line density J_{01}^{line} from v_s and L_{diff} measured by LBIC, the obtained values are a factor of about 1.7 in the case of sample A respectively 3.4 for sample B lower than measured by DLIT. This indicates that there are additional sources of recombination caused by the grain boundary, which are not included in the underlying models of the methods.

Table III: Recombination parameters obtained from both evaluation methods at the grain boundaries presented in Fig. 2. Note that due to the exponential dependency of v_s on J_{01}^{line} the error range is not symmetrical.

Sample		LBIC	DLIT
A	L_{diff} [mm]	1 … 3	0.7 … 1.1
	v_s [cm/s]	2×10^4	6.2×10^5
	error range		3.7×10^5 … 11.2×10^5
B	L_{diff} [mm]	0.4 … 0.6	0.17 … 0.19
	v_s [cm/s]	1.4×10^5	1.8×10^{10}
	error range		0.8×10^{10} … 4.1×10^{10}

5 DISCUSSION

Section 4 exposes that although the two presented analysis methods are based on similar models, there are discrepancies in the evaluated values of the minority carrier diffusion length and the surface recombination velocity at the grain boundaries. There are several issues that have to be taken into account, if the two measurements are compared to each other.

The most important difference between the two methods is the kind of excitation of the solar cell. The LBIC measurement illuminates the solar cell with a laser spot, which generates the carriers within the bulk. Different laser wavelengths used enable the generation of carriers in different depth of the semiconductor and thus provide a quite good determination of the diffusion length L_{diff} due to the different path of the carriers towards the p-n junction and the contacts, where they are measured. Operating in short circuit condition guarantees a maximal collection efficiency of the emitter, which is

used in conjunction to laser wavelength with penetration depths significantly larger than the emitter thickness but also significantly smaller than the cell thickness. Thus the result is almost unaffected by the recombination at the surfaces of the solar cell, but comes only from the recombination properties of the bulk. In such defined conditions the used model assumes an infinitely thick solar cell with neglected depletion region and emitter [6]. The used samples are about 350 µm thick and thus provide an independent evaluation of L_{diff}.

While measuring with DLIT the cell is biases in the dark and thus the minority carrier concentration at the p-n junction is constant. The necessary additional current density to keep this status, when minority carriers recombine, is directly measured. This recombination can take place in the bulk as well as in the depletion region, the emitter or at the surfaces. High resolution DLIT cannot decide where in the depth the recombination takes place, but summarizes all influences of the GB on the solar cell performance. Edmiston et al. [11] describe an increased recombination current density with an ideality factor of 1.8 when the GB passes the p-n junction, which is not negligible in case of high recombination activity. Thus the used model is just a poor description of the measured phenomena, and this might be the first reason, why the DLIT analysis calculates higher values than the LBIC measurement.

For the same reason the measured diffusion length is lower than the bulk value L_{diff}, which can be evaluated quite well by LBIC. The DLIT analysis evaluates current densities and thus an effective lifetime, which is influenced by the bulk properties as well as by the surface recombination and so on. Especially since L_{diff} is larger than the thickness of the investigated solar cells, there is a significant influence of the surface recombination on the effective lifetime τ_{eff}. The effective diffusion length, which is defined on base of this τ_{eff}, therefore is not able to describe the diffusion of the minority carriers in the grain and might cause additional downscaling of v_s according to equation (1).

Another difference is the analysis of the detected signal. The LBIC signal is normalized to a contrast profile and thus all spatially homogeneous parts of the recombination in the emitter or at the surfaces, which still might slightly influence the measured signal will be obliterated. In contrast to that the DLIT signal first has to be spatially deconvoluted in order to obtain the necessary spatial resolution. As it is visible in Figures 1 and 2 the thermal damping of the gridlines cannot be considered and thus results in low or even negative values. As in the most quantitative DLIT analysis the conversion from thermal information to power information is done by a normalization of the overall thermal signal to the overall power density ($I*V$) [7]. Due to the negative data the measured values might be slightly too high, but since the areal fraction of the grid lines is quite small, it has a minor significance.

Due to the high spatial resolution the fitting of the LBIC contrast profiles is targeted on the whole shape of the curves and thus uses all given information. The DLIT analysis uses just integral values, since the original data are thermally blurred and thus the shape information is mainly influenced by the deconvolution algorithm. For this reason the LBIC procedure reveals much more exact values and does not depend on additional data as the doping of the sample N_A. This parameter can significantly change the results. For example, a decrease to about 6×10^{15} cm^{-3} would reduce v_s in sample A by more than one order of magnitude. We evaluate N_A from resistivity measurements at the wafer and thus the N_A cannot be lower than the given value, because a lower mobility than assumed would rather increase the N_A and thus would raise the evaluated v_s.

According to [12] there also might be an injection level dependency of the surface recombination velocity of GBs even in low injection regimes. Both methods work in low injection regimes: LBIC injects about 3×10^{13} cm^{-3} within the laser spot and DLIT provides about 7 to 10×10^{13} cm^{-3} at the p-n junction. Since v_s becomes lower with increasing excitation, this is in contrast to the observations made here, but has to be considered for a deeper interpretation of results obtained from different measurements.

The last point concerns the recombination in other parts of the solar cells than in the bulk. The depletion region recombination current is neglected in both evaluation methods. Since there is a decrease of the averaged depletion region recombination current in the center of the solar cell due to the hydrogenation (sample A vs. B), even the GBs might cause some additional j_{rec}. The interpretation of a solely diffusion current density as done in the DLIT analysis might cause also errors as the missing description of such a phenomena in the models.

It has to be mentioned that both methods also disregard the recombination at the front and the rear side of the solar cell. Previous works based on CELLO [13] and DLIT [14] have shown that crystal defects, which limit the effective lifetime in the bulk, might also increase the recombination at the rear side and in the emitter. This fact will be considered by the methods in different manner. Since LBIC is not sensitive for such additional recombination at the rear side, not just the evaluation of the diffusion length in the grain but also the J_{01}^{line} might be influenced by the rear side recombination and might be larger than measured by LBIC. Thus the DLIT measurement represents all recombination phenomena caused by the GB and thus estimates their influence on the cell performance, while the LBIC measurement just points to the bulk effects. Moreover, the DLIT evaluation assumes that the diffusion current is dominated by j_{01}^{bulk}. In reality, the measured dark current density also contains $j_{01}^{emitter}$.

All the above mentioned data might consider the differences of both measurements on sample A, but sample B shows the limitations of the DLIT-based procedure. All measured values are much higher than estimated from the results given by the LBIC method. Due to the missing H-passivation significant recombination takes place at more places than implemented in the simple model and thus the calculation of a surface recombination velocity to describe the recombination activity of the GB is not possible by means of DLIT. The value obtained from LBIC just represents a part of the overall recombination effects caused by this crystal defect.

6 CONCLUSION

There are two different kinds of methods, which expose the recombination at grain boundaries in mc solar cells. Their main advantages and limitations are explicitly discussed in section 5 and summarized in Table IV.

Although both methods are based on almost the same model of an infinitely thick solar cell with neglected recombination in the emitter and the depletion region, there are significant differences due to the different ways of excitation. Only the LBIC procedure confirms quite well to this model, but the DLIT method directly measures the additional current due to the different recombination paths caused by the GB and thus estimates better its total influence on the cell performance.

Especially high diffusion lengths are hardly measurable with the DLIT method, but can have a significant influence on the result. In contrast to that the result of the LBIC method is not sensitive for very high L_{diff}, since the collection efficiency approaches unity and thus the contrast profile does not change significantly.

Another limitation is the exponential dependency of v_s on J_{01}^{line}, which regards very urgent errors in evaluating large surface recombination velocities of the GB. Additionally, the carrier transport from two different grains through a minor active GB can only be fitted correctly by the LBIC method.

Table IV: Advantages (+) and limitations (–) of both methods based on LBIC and DLIT (o = neutral).

LBIC			DLIT
• fitting the shape of the whole contrast profile	o	o	• integral value of the additional current
• direct evaluation of L_{diff}	+	–	• evaluation of L_{eff}
• high spatial resolution	+	–	• image deconvolution
• not sensitive for errors of high L_{diff}	+	–	• problems in measuring very high L_{diff}
• not sensitive for surface effects of the GB	–	+	• summarizes all recombination effects at GB
• different properties of adjacent grains fitable	+	–	• symmetric GB or high v_s (one side fit)

Thus it can be summarized that the LBIC-based method has a much broader adaptability, but the DLIT-based version concerns all recombination effects at the GB via a direct dark current measurement and thus gives a better estimation of the influence on the cell performance, while LBIC just looks at one part of it.

ACKNOWLEDGEMENTS

This work was financially supported by the German Federal Ministry for Environment, Nature Conservation and Nuclear Safety and by industry partners within the research cluster "SolarWinS" (contracts no. 0325270C and 0325270F). The content is the responsibility of the authors.

REFERENCES

[1] G. Micard, G. Hahn, A. Zuschlag, S. Seren, B. Terheiden, Journal of Applied Physics 108 (2010) 034516.
[2] S. Rißland, O. Breitenstein, Solar Energy Materials and Solar Cells 104 (2012) 121.
[3] S. Rißland, O. Breitenstein, Energy Procedia 38 (2013) 161.
[4] A. Zuschlag, G. Micard, J. Junge, M. Käs. S. Seren, G. Hahn, G. Coletti, G. Jia, W. Seifert, Proceedings of the 33rd IEEE Photovoltaic Specialists Conference, San Diego, USA (2008).
[5] K. Ramspeck, K. Bothe, D. Hinken, B. Fischer, J. Schmidt, R. Brendel, Applied Physics Letters 90 (2007) 153502.
[6] C. Donolato, Journal of Applied Physics 54 (1983) 1314.
[7] O. Breitenstein, W. Warta, M. Langenkamp, „Lock-in Thermography“, 2nd edition, Springer Series in Advanced Microelectronics, Berlin, Springer Verlag (2010).
[8] O. Breitenstein, Solar Energy Materials and Solar Cells 95 (2011) 2933.
[9] O. Breitenstein, A. Khanna, Y. Augarten, J. Bauer, J.-M. Wagner, K. Iwig, Physica Status Solidi RRL 4 (2010) 7.
[10] M. Lax, Journal of Applied Physics 48 (1978) 2796.
[11] S.A. Edmiston, G. Heidser, A.B. Sproul, M.A. Green, Journal of Applied Physics 80 (1996) 6783.
[12] J. Qualid, C.M. Singal, J. Dugas, J.P. Crest, H. Amzil, Journal of Applied Physics 55 (1984) 1195.
[13] J. Carstensen, A. Schütt, G. Popkirov, H. Föll, Physica Status Solidi C 8 (2011) 1342.
[14] S. Rißland, T.M. Pletzer, H. Windgassen, O. Breitenstein, IEEE Journal of Photovoltaics 3 (2013), 1192.